Effects of mPEG Grafts on Morphology and Cross-Linking of Thermally Induced Micellar Assemblies from PAAc-Based Graft Copolymers in Aqueous Phase

Wen-Hsuan Chiang,[†] Yuan-Hung Hsu,[†] Tzu-Wei Lou,[†] Chorng-Shyan Chern,[‡] and Hsin-Cheng Chiu*,[†]

Department of Chemical Engineering, National Chung Hsing University, Taichung 402, Taiwan, and Department of Chemical Engineering, National Taiwan University of Science and Technology, Taipei 106, Taiwan

Received February 5, 2009; Revised Manuscript Received March 30, 2009

ABSTRACT: Two graft copolymers comprising acrylic acid (AAc) and 2-methacryloylethyl acrylate (MEA) units as the backbone and either poly(*N*-isopropylacrylamide) (PNIPAAm) alone or both PNIPAAm and monomethoxypoly(ethylene glycol) (mPEG) as the grafts were synthesized. These copolymers in the aqueous phase (pH 5.0) underwent thermally induced self-assembly into micelles. For the copolymer containing PNIPAAm grafts only, extensive interactions between un-ionized AAc residues and PNIPAAm segments occurred, thereby rendering polymer backbones partially embedded within the hydrophobic cores of thermally induced micelles. This then led to bulk (core/shell) cross-linking of micelles upon radical polymerization of the MEA units within the micellar assemblies in the aqueous phase. By contrast, with mPEG being incorporated into the copolymer, association of the backbones with PNIPAAm is greatly retarded. As a result, three-layer onion-like polymeric micelles consisting of hydrophobic PNIPAAm cores surrounded by AAc-rich shells and hydrophilic mPEG coronas were achieved. Shell cross-linked micelles were then produced via polymerization of the MEA units confined to the AAc/MEA-rich shell regions. The presence or absence of mPEG in the PNIPAAm-containing graft copolymer plays a crucial role in determining the morphological structure of micelles and the structural responses of the subsequently cross-linked micelles to pH and temperature changes.

Introduction

Micellar assemblies obtained from double hydrophilic block or graft copolymers containing pH- or thermo-responsive chain segments are of great fundamental interest and industrial importance owing to their unique structural characteristics and potential applications in drug delivery, protein immobilization, interface mediators and catalysis.[1–5] Growing attention has also been paid to the processes of formation, disintegration and structural (core/shell) inversion and transition of polymeric micelles in response to external stimuli such as temperature, pH and ionic strength.[6–8] However, due to fast disintegration of polymeric micelles upon changes in pH and/or temperature and dilution in blood circulation after parenteral administration, their practical applications in drug delivery are severely limited. In order to attain morphologically stable polymeric micelles while retaining full reversibility in stimuli-responsive processes, both the core cross-linking (CCL)[9–14] and shell cross-linking (SCL)[15–25] approaches have been explored extensively.

For example, Wooley and co-workers have prepared various CCL micelles in aqueous phase by a "click" core cross-linking of polystyrene (PS)-*b*-PAAc, which contains alkynyl residues within the hydrophobic PS block with dendrimers of different generations.[13] Zhang et al. proposed a facile approach to attain CCL micelles from a double hydrophilic block copolymer, PEG-*b*-P(NIPAAm-*co*-*N*-acryloxysuccinimide (NAS)), which spontaneously assembles into micelles in aqueous solution at high temperature.[14] Using cystamine as the cross-linker to react with NAS residues of the P(NIPAAm-*co*-NAS) block results in temperature-responsive CCL micelles.

The SCL technique provides another pathway for stabilization of polymeric micelles. Armes and co-workers prepared SCL micelles by using a diblock copolymer of (2-(*N*-(morpholino)-ethylmethacryate) and 2-(dimethylamino)ethylmethacrylate) (DMA) in aqueous solution at 60 °C. The reagent 1,2-bis(2-iodoethoxy)ethane was used to selectively cross-link the DMA residues residing within the inner shells of micelles.[15] Another example for the formation of SCL micelles is the condensation of ethylenediamine with the reactive NAS residues of PEG-*b*-P(*N*,*N*-dimethylacrylamide-*s*-NAS)-*b*-PNIPAAm) triblock copolymer in aqueous media at elevated temperature. The resultant SCL micelles exhibited the capability of controlling their swelling behavior via the response to temperature change.[24] Dou et al. prepared micelles from the PAAc grafted hydroxyethyl-cellulose (HEC) at low pH by the complexation of HEC with PAAc as hydrophobic cores while free HEC backbone segments act as hydrophilic shells.[25] Upon cross-linking of PAAc segments in micelles, the stabilized assemblies become capable of undergoing reversible pH-induced morphological transition from micelles to hollow spheres.

In this work, two graft copolymers comprising AAc and MEA residues as the backbone and either PNIPAAm alone or both PNIPAAm and mPEG as the grafts were synthesized and characterized. By comparing with the assemblies produced by the graft copolymer in the absence of mPEG grafts, the effects of mPEG chains on regulating both the structures of the thermally induced polymeric micelles and the responses of CL micelles achieved by free radical polymerization of the MEA residues to pH and temperature changes were investigated in this work.

Experimental Section

Materials. Synthesis and characterization of PNAS and aminated semitelechelic PNIPAAm (PNIPAAm−NH₂) (3000 g/mol) and mPEG (mPEG−NH₂) (2000 g/mol) were described in our previous

---

* To whom correspondence should be addressed. Fax: 886-422854734. Telephone: 886-422852636. E-mail: hcchiu@dragon.nchu.edu.tw.
† Department of Chemical Engineering, National Chung Hsing University.
‡ Department of Chemical Engineering, National Taiwan University of Science and Technology.

Scheme 1. Synthetic Route and Chemical Structure of Graft Copolymer B
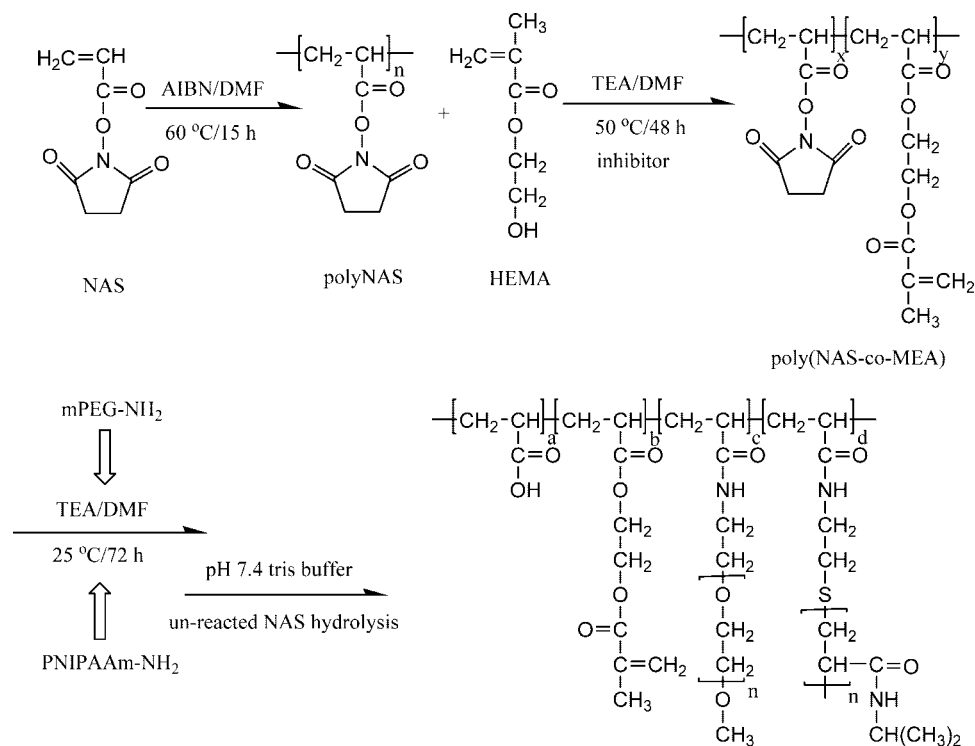
work.[26,27] Ammonium peroxydisulfate (APS) was obtained from Showa (Tokyo, Japan). 2-Hydroxyethyl methacrylate (HEMA) and 1-pyrenemethylamine hydrochloride were obtained from Aldrich (WIS, USA). HEMA was purified by extraction and distillation under reduced pressure before use.[28] Deuterium solvents used in ^{1}H NMR measurements were obtained from Cambridge Isotope (MA, USA). Deionized water was produced from Milli-Q Synthesis (18 MΩ, Millipore). All other chemicals are reagent grade and used as received.

Copolymer Synthesis. Incorporation of vinyl groups into PNAS was performed by partial transesterification of PNAS with HEMA and the resultant intermediate product was P(NAS-*co*-MEA). The procedure is briefly described as follows. To a solution of PNAS (10.0 g) in DMF (100 mL) in the presence of triethylamine (TEA) (600 mg) as the catalyst and 2,6-di-*tert*-butyl-4-methylphenol (5.0 mg) as the radical polymerization inhibitor, a prescribed amount of HEMA (10 mol % with respect to the initial NAS residues) was added and the reaction was conducted at 50 °C for 48 h under stirring. The product was purified by precipitation twice from excess *tert*-butyl alcohol and collected by filtration. The conjugation extent of HEMA was determined by ^{1}H NMR spectroscopy (Varian Unity Inova-600, 600 MHz) in DMSO-d_6 at ambient temperature.

Grafting reactions of P(NAS-*co*-MEA) (10% w/v) in DMF with PNIPAAm−NH$_2$ alone (10 mol % with respect to the NAS residues of PNAS (referred to as copolymer **A** hereinafter)) and with both PNIPAAm−NH$_2$ and mPEG−NH$_2$ (10 mol % each, copolymer **B**), respectively, were carried out at 25 °C under stirring for 72 h. TEA was used as the catalyst. The synthetic route of copolymer **B** is illustrated in Scheme 1. In order to examine the micellar structure, the copolymer backbones were chemically labeled with pyrene by the reaction of 1-pyrenemethylamine hydrochloride (0.3 mol % with respect to the original NAS residues) with the NAS residues of P(NAS-*co*-MEA) prior to the grafting reactions of the copolymer with PNIPAAm−NH$_2$ and mPEG−NH$_2$ (Supporting Information). The pyrene-labeled copolymers **A** and **B** are referred to as copolymers **A** (Py) and **B** (Py), respectively, hereinafter. The unreacted NAS residues in graft copolymers were thoroughly hydrolyzed to AAc units by addition of excess tris buffer (pH 7.4) into the reaction media. The polymer solution was then dialyzed (Spectra/Por MWCO 6000−8000) against deionized water for 7

days to remove DMF and *N*-hydroxysuccinimide. This was followed by diafiltration (Millipore, Labscale TFF System equipped with Pellicon XL membrane Biomax-30 MWCO 30000) to eliminate, in a more efficient manner, unreacted PNIPAAm and, in the case of copolymer **B**, mPEG as well. The final products were collected by lyophilization and the compositions determined by ^{1}H NMR in DMSO-d_6 at 20 °C. The conjugation extent of pyrene was quantitatively determined by UV/vis spectrometer (Shimadzu UV-1601).[29]

CL Micelle Preparation. The graft copolymer (**A** or **B**) was dissolved to a concentration of 10.0 mg/mL in acetate buffer (pH 5.0, *I* 0.01 M) at 4 °C. The polymer solution was subsequently passed through a 0.45 μm filter and purged with N$_2$ for 30 min. It was gradually heated to 60 °C and equilibrated at this temperature with stirring (100 rpm of the reciprocal shaking) for 12 h. Vigorous agitation is required thus to prevent formation of intermicellar aggregates. CL micelles were prepared by radical polymerization of the MEA residues of copolymer **A** or **B** in micelle form for 72 h, using APS (0.6 mg/mL) as the initiator. The CL micelle solution was then subjected to ultrafiltration (Amicon 8200 with a Millipore PBMK membrane, MWCO 300000) against the acetate buffer at ambient temperature to remove copolymers that were not cross-linked.

UV/Vis Transmittance Measurements. Transmittance measurements of the copolymer solutions (10.0 mg/mL) with varying pH were conducted on a Shimadzu UV-1601 spectrometer at a wavelength of 600 nm equipped with a temperature-controlled cell unit. The optical transmittance was recorded with temperature in the range 20−60 °C. The sample cell was equilibrated at each preset temperature for 10 min prior to measurements.[30]

Fluorescence Measurements. Pyrene, both in free molecule form and in conjugated form with copolymer backbones, was used as a nonpolar probe in the fluorescence characterization of aqueous copolymer solutions. In the latter case, the fluorescence emission spectra were recorded for the aqueous solutions of copolymers **A** (Py) and **B** (Py) (10.0 mg/mL) of varying pH (*I* 0.01, adjusted by NaCl). In the former case, in which free pyrene was used, aliquots (20.0 μL) of the pyrene solution (3.0 × 10^{-5} M) in acetone were evaporated in vials, followed by addition of the aqueous copolymer solution (10.0 mg/mL, 1.0 mL; *I* 0.01). The resultant sample was

kept at 4 °C for 12 h, thereby leading to the polymer solution with a constant pyrene concentration of ca. 6.0×10^{-7} M. Fluorescence characterization was performed by measuring the fluorescence intensity ratios (I_3/I_1) of the third vibronic band at 385.5 nm to the first at 373.5 nm of the fluorescence emission spectra of pyrene in aqueous copolymer solutions as a function of temperature.[31] The excitation was induced at 336 nm and the emission was recorded in the range 350−500 nm on a Hitachi F-2500 fluorescence spectrometer equipped with a thermostat cell unit.

^{1}H NMR Characterization. Graft copolymer (**A** or **B**) was dissolved in D_2O (0.01 M NaCl) to a final concentration of 10.0 mg/mL while the pD of the copolymer solutions was adjusted to 5.0 by NaOD. The variable-temperature ^{1}H NMR was conducted on a Varian Unity Inova-600 at 600 MHz without sample spinning. The pulse width of 4.9 μs with a relaxation delay of 2.0 s was utilized. During ^{1}H NMR measurements, DMF in a sealed capillary was coaxially placed in the sample tube as an external standard, and its signal at δ 8.45 ppm selected as reference resonance for evaluating the feature signal integrals of the graft copolymers in response to temperature change in comparison with those in DMSO-d_6 at ambient temperature.[26,27] The sample was equilibrated at each preset temperature for 30 min prior to measurement.

Dynamic Light Scattering (DLS) Measurements. The mean hydrodynamic diameters (D_h) of micelles and CL micelles were determined by a Malvern ZetaSizer Nano Series instrument (He−Ne laser 4 mW, λ = 633 nm). The aqueous copolymer solution was passed through a 0.45 μm filter at 20 °C and equilibrated at either 20 or 60 °C for 30 min with stirring prior to measurement. The measurement at 60 °C was performed immediately to prevent micelles from aggregating with one another. The mean particle sizes of the CL micelle systems were determined in the temperature range 20−60 °C at varying pH adjusted by either 0.1 N NaOH or HCl. The sample was equilibrated at each preset temperature for 30 min. The results reported herein represent an average of at least triplicate measurements.

TEM Examination. The sample was prepared by placing a few drops of the CL micelle solution on a 300-mesh copper grid covered with carbon and allowed to stand at 25 °C for 20 s. Excess solution on the grid was gently removed with absorbent paper. This is followed by negative staining of the sample by using a uranyl acetate solution (5.0 wt %) for 20 s. The sample was then dried at 25 °C for 2 days. The TEM image was obtained on a JEOL JEM-1200 CXII microscope operating at an accelerating voltage of 120 kV.

Results and Discussion

Copolymer Composition Characterization. As shown in the ^{1}H NMR spectrum (Figure 1a), the MEA content of P(NAS-*co*-MEA) was evaluated to be ca. 9.2 mol % based on the signal integral ratio $x/(x + y/4) \times 100\%$. The parameter x represents the average integral of the protons attached to the carbon−carbon double bond of MEA at δ 5.7 and 6.1 ppm and y the integral of the succinimidyl protons of NAS at δ 2.8 ppm. With the efficiency being greater than 90%, the transesterification reaction can thus be achieved in a fully controllable manner. The ^{1}H NMR spectra of copolymers **A** and **B** in DMSO-d_6 are shown in Figure 1, parts b and c, respectively. On the basis of the assignment of the ^{1}H NMR spectrum shown in Figure 1c, the composition of copolymer **B**, for example, can be calculated as follows:

$$\text{MEA (9.2 mol \%)·PNIPAAm (} a \text{ mol \%)·mPEG(} b \text{ mol \%)} =$$
$$p : \frac{q}{(M_{w,\text{PNIPAAm}}/113) \times 6} : \frac{r}{(M_{w,\text{PNIPAAm}}/44) \times 4}$$

where a and b represent the contents in mol % of the PNIPAAm and mPEG grafts and p, q and r are the feature signal integrals obtained from MEA (the average integral of protons attached to the double bond at δ 5.7 and 6.1 ppm), PNIPAAm (the methyl protons at 1.1 ppm) and mPEG (the ethylene protons at 3.8
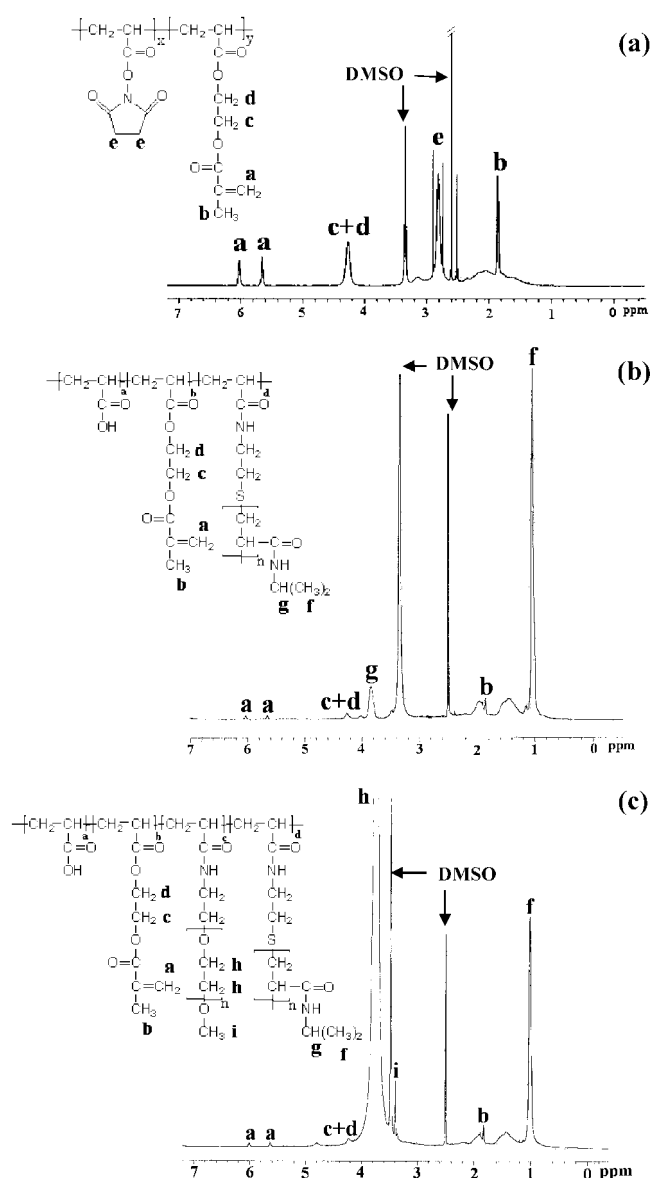

Figure 1. ^{1}H NMR spectra of (a) poly(NAS-*co*-MEA), (b) graft copolymer **A** and (c) graft copolymer **B** in DMSO-d_6 at 20 °C.

Table 1. Recipes, Compositions, and Average Molecular Weights of the Graft Copolymers

copolymer	reaction feed (mol %) NAS/MEA/pyrene/ PNIPAAm/mPEG	composition ratio[a] (mol %) AAc/MEA/pyrene/ PNIPAAm/mPEG	$M_w{}^{b}$ ($\pm 10^{-5}$ g/mol)
A	100/10/0/10/0	84.9/9.2/0/6.0/0	0.78
A(Py)	100/10/0.3/10/0	84.54/9.2/0.26/6.0/0	0.78
B	100/10/0/10/10	79.1/9.2/0/5.5/6.9	1.15
B(Py)	100/10/0.3/10/10	78.14/9.2/0.26/5.5/6.9	1.15

[a] Determined by ^{1}H NMR measurements in DMSO-d_6. [b] Obtained by theoretical calculations as follows: backbone M_w 22000 (g/mol) (M_w of PAAc by the GPC measurement after thorough hydrolysis of PNAS)[26] + number of mPEG grafts × 2000 (M_w of mPEG) + number of PNIPAAm grafts × 3000 (M_w of PNIPAAm) + number of MEA residues × 113 (M_w of MEA).

ppm), respectively. The grafting efficiencies for both PNIPAAm and mPEG were ca. 60%. The recipes, compositions and average molecular weights of the graft copolymers are summarized in Table 1. Note that the Michael type addition reaction, which can presumably occur between primary amines of PNIPAAm−NH_2 or mPEG−NH_2 with vinyl groups of MEA residues during the grafting reactions, was not observed, as evidenced by the essentially identical MEA contents in graft copolymers before
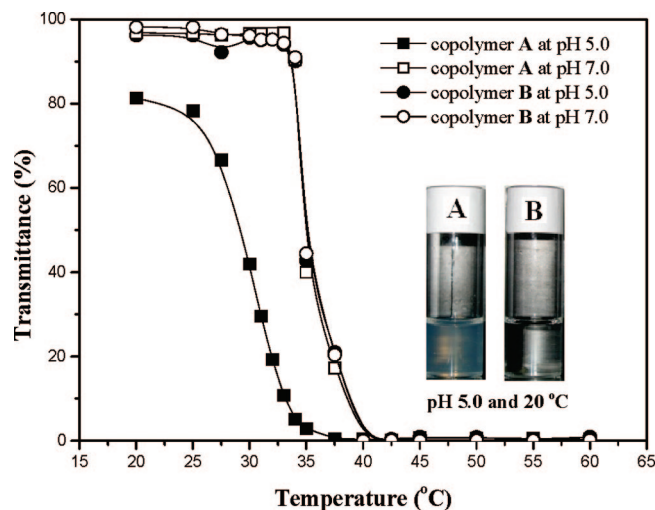
Figure 2. Temperature dependence of the optical transmittance for aqueous solutions of copolymers **A** and **B** (10.0 mg/mL) at pH 5.0 and 7.0. The inset shows the photographs of aqueous solutions of copolymers **A** and **B** (10.0 mg/mL) at pH 5.0 and 20 °C.

and after grafting reactions. The data are shown in Supporting Information. Obviously, as a result of the facile reactivity and high concentration of succinimidyl ester, it is much preferable for both PNIPAAm−NH$_2$ and mPEG−NH$_2$ to react with the NAS residues instead of the vinyl groups of MEA units.

Micelle Formation Mechanisms. Owing to the inherent lower critical solution temperature (LCST) of PNIPAAm,[7,14,24] both copolymers **A** and **B** undergo phase transition and supramolecular assembly into micellar structure in the aqueous phase upon the thermally induced hydrophobic association of the PNIPAAm grafts, as illustrated by the optical transmittance data in Figure 2. Phase transition of the aqueous solutions (10.0 mg/mL) of copolymers **A** (pH 7.0) and **B** (pH 5.0 and 7.0) occurs abruptly in the temperature range 32−35 °C. However, in the absence of mPEG grafts, copolymer **A** at pH 5.0 undergoes phase separation in a progressive manner at temperature far below the LCST of PNIPAAm (ca. 32 °C). This is caused primarily by the enhanced hydrogen-bond induced hydrophobic association of polymeric segments.[32,33] Complementary pairings of AAc with NIPAAm residues via hydrogen bonds originating from PAAc and PNIPAAm segments, respectively, have been well documented.[7,32−35] These hydrogen bonds are largely disrupted and, consequently, the hydrophobic association between PAAc and PNIPAAm segments becomes markedly reduced as a result of the increased AAc ionization with pH being increased from 5.0 to 7.0. This will then lead to a shift of the phase transition temperature to 32−35 °C for copolymer **A**, similar to that of PNIPAAm alone in the aqueous phase. Interestingly enough, copolymer **B** that differs from **A** simply in the presence of mPEG grafts shows a temperature-evolved, but pH-independent phase transition behavior. The dramatic difference between the solutions of copolymers **A** and **B** at pH 5.0 and 20 °C is illustrated in Figure 2. Apparently, the mPEG grafts in copolymer **B** play a crucial role in prohibiting the formation of hydrophobic PAAc/PNIPAAm complexes at low temperature.

In agreement with the optical transmittance data in Figure 2, the DLS data indicate that both graft copolymers subjected to heating from 20 to 60 °C at varying pH undergo significant changes in colloidal particle size (D_h) and size distribution (PDI) and so does the intensity of light scattering (Table 2). While copolymers **A** at pH 7.0 and **B** at both pH 7.0 and 5.0 were completely dissolved in aqueous solution at 20 °C, copolymer **A** at pH 5.0 existed in aggregate state. The copolymers with

Table 2. Mean Hydrodynamic Diameters (D_h) and Polydispersity Indices (PDI) of Graft Copolymers A and B (10.0 mg/mL) in Aqueous Solutions at pH 5.0 and 7.0

		20 °C		60 °C	
	pH	D_h (nm)	PDI	D_h (nm)	PDI
A	5.0	53.0 ± 4.5 (27.2)[a]	0.43 ± 0.02	73.1 ± 3.8 (67.4)	0.16 ± 0.01
	7.0	18.3 ± 2.4 (0.8)	0.53 ± 0.03	410.2 ± 10.8 (4.9)	0.22 ± 0.02
B	5.0	15.5 ± 3.6 (2.1)	0.41 ± 0.04	50.2 ± 2.6 (15.0)	0.23 ± 0.01
	7.0	17.9 ± 1.5(1.1)	0.43 ± 0.03	350.3 ± 10.3 (3.4)	0.25 ± 0.02

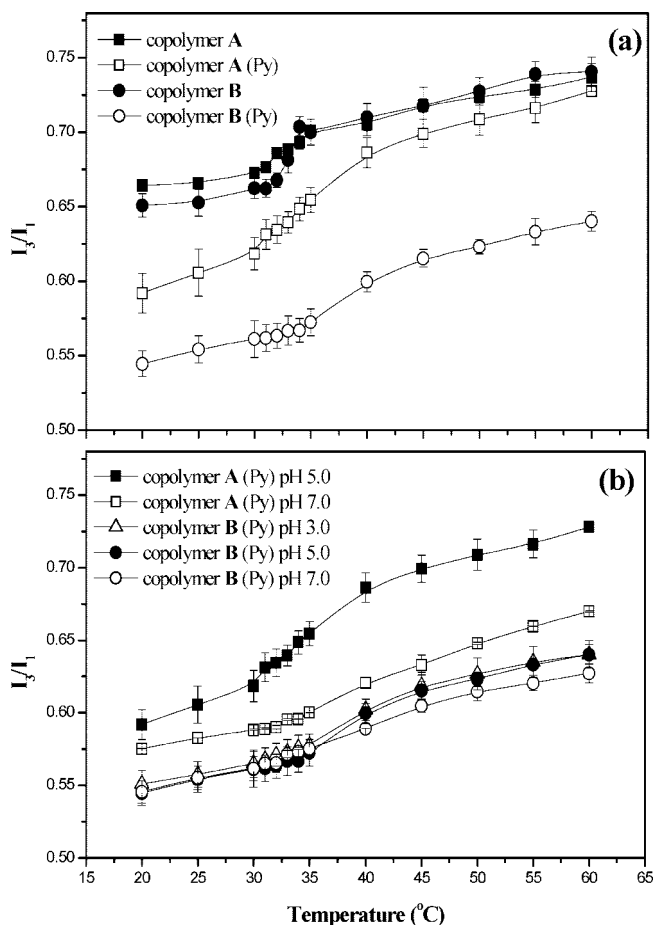[a] Numeric values in parentheses are the light scattering intensity of DLS measurements in Mcps.

Figure 3. Temperature dependence of the fluorescence intensity ratio I_3/I_1 for aqueous solutions of copolymers **A** and **B** (free pyrene was used) and copolymers **A** (Py) and **B** (Py) (10.0 mg/mL) at pH 5.0 (a) and at varying pH (b). Error bars represent the standard deviation of triplicate measurements.

the enhanced extents of AAc ionization at pH 7.0 underwent the thermally induced supramolecular packing into colloidal assemblies of relatively large size (D_h = 350−410 nm) due to extensive multicore structure and intercore connections within the assemblies.[26] The TEM images of the assemblies at pH 7.0 and 60 °C are included in Supporting Information. At pH 5.0, both copolymers **A** and **B**, while experiencing a temperature change from 25 to 60 °C, are transformed into micellar assemblies, in which the inner core comprises mainly hydrophobic PNIPAAm segments, regardless of the very different colloidal structures of these two copolymers at ambient temperature, as shown in Figure 2 and Table 2.

Fluorescence characterization of the aqueous copolymer solutions at pH 5.0, using free pyrene as a nonpolar probe, confirms that the assembly process is driven by thermally induced hydrophobic association, as illustrated by a substantial increase in the fluorescence intensity ratios (I_3/I_1) of pyrene in
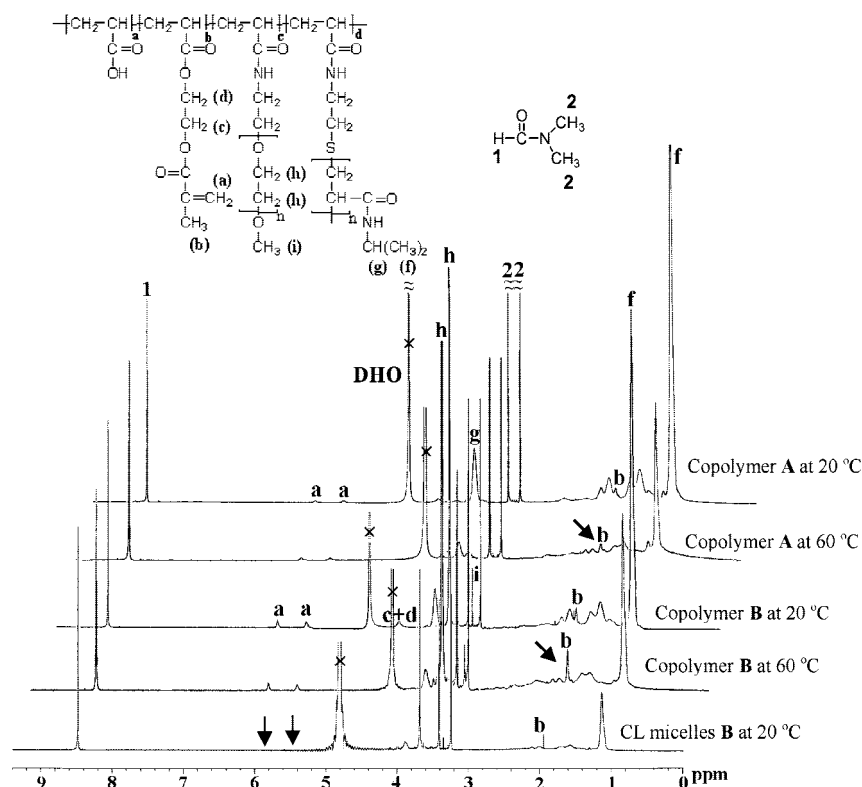
Figure 4. ¹H NMR spectra of copolymers **A** and **B** (10.0 mg/mL) in D₂O (pD 5.0) at 20 and 60 °C and CL micelles **B** (2.0 mg/mL) at 20 °C, using the DMF signal at 8.45 ppm as an external reference.
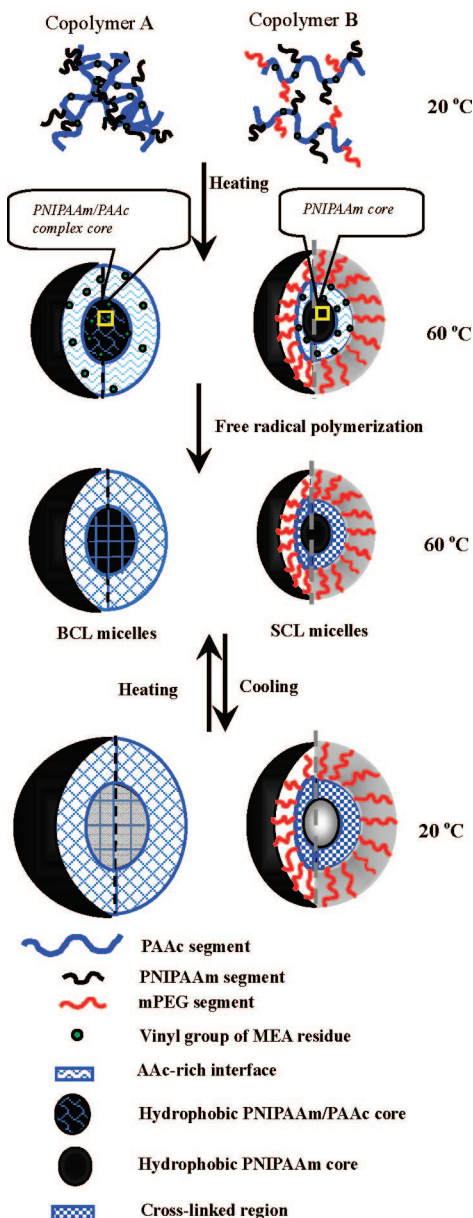
the temperature range 30−35 °C (Figure 3a). The intensity ratio represents a quantitative measure of the nonpolar nature of the microenvironments, in which pyrene resides. Because of its inherent nonpolar nature, pyrene molecules tend to diffuse to the most hydrophobic regions in aqueous polymer solution. By contrast, the mobility of pyrene moieties covalently labeled onto polymeric backbones is severely limited and, thus, the I_3/I_1 value reflects the hydrophobicity of the environment where polymer backbones are associated. Several studies also monitored assembling of amphiphilic copolymers by the transition of labeled pyrene residues from polar to nonpolar media.[36,37] As expected, only a slightly higher I_3/I_1 value of free pyrene in the aqueous solution of copolymer **A** at pH 5.0 and 20 °C than that of the counterpart **B** was observed (see the solid square and circular data points in Figure 3a). However, when pyrene was covalently attached to polymeric AAc/MEA backbones, the difference that accounts for more precisely the variation in the hydrophobicity of backbones between copolymers **A** and **B** at ambient temperature becomes significant due to enhanced pairings of un-ionized AAc with NIPAAm units for copolymer **A** (see the open square and circular data points in Figure 3a). With the temperature being raised beyond the phase transition of copolymers, insignificant difference in the I_3/I_1 values of free pyrene between copolymers **A** and **B** is observed. This implies a similar structure of the most hydrophobic regions of micelles **A** and **B**. More importantly, the much higher I_3/I_1 values of copolymer **A** (Py) than those of **B** (Py) at high temperature strongly suggest that the hydrogen bonds between un-ionized AAc and NIPAAm residues at pH 5.0 remain intact toward the temperature rise beyond the phase transition of copolymer, thereby leading to association of partial polymer backbones within the hydrophobic PNIPAAm cores of micelles. By contrast, as shown by the I_3/I_1 profile for copolymer **B** (Py) in Figure 3a, polymer backbones comprising mainly AAc and MEA residues are mostly separated from the hydrophobic cores of micelles almost entirely consisting of PNIPAAm grafts. This

signifies that mPEG grafts in copolymer **B** can prevent polymer backbones from being embedded into hydrophobic PNIPAAm cores at high temperature and, thereby, confine those polymerizable MEA moieties mostly in the AAc-rich interfacial layers (shells) between inner hydrophobic PNIPAAm cores and outer hydrated mPEG coronas of micelles.

The above postulation can be further confirmed by the I_3/I_1 data for copolymers **A** (Py) and **B** (Py), at various pH. As shown in Figure 3b, the I_3/I_1-temperature profile for copolymer **B** (Py) is rather independent of the medium pH (3.0, 5.0 and 7.0) because pairings of un-ionized PAAc with PNIPAAm can be greatly prohibited by mPEG grafts. While extensive interactions occur via hydrogen bonds between un-ionized AAc and NIPAAm residues at pH 5.0, thereby rendering partial backbones embedded within hydrophobic cores of micelles **A** beyond the phase transition temperature, these interactions are largely disrupted by adjusting pH from 5.0 to 7.0 as a result of an increase in the AAc ionization extent. Note that the data for copolymer **A** at pH 3.0 were not included in Figure 3b due to the precipitation of colloidal particles at high temperature.

The potentiometric titration profiles for copolymers **A** and **B** are almost identical (Supporting Information) and, therefore, the effect of mPEG grafts on the ionization of the backbone AAc units is negligible. While the dissociation degrees of AAc residues for both copolymers at pH 7.0 and 25 °C were ca. 47%, the ionization extent at pH 5.0 was reduced to only ca. 10%. Under this circumstance, un-ionized AAc/NIPAAm pairings can occur appreciably for copolymer **A** in the absence of mPEG grafts. PEG is well-known for its unique amphiphilic property and the steric stabilization available for preventing colloidal particles from aggregation in the aqueous phase. The consecutive pairings of un-ionized AAc with NIPAAm residues that greatly promote the hydrophobic association of polymer chain segments can be sterically hindered to some extent by the mPEG grafts attached to polymer backbones. In addition, this steric hindrance effect can be ascribed in part to the preferred residence of mPEG

Scheme 2. Structure and Cross-Linking of Thermally Induced Micelles from Graft Copolymers A and B (10.0 mg/mL) in Aqueous Solutions of pH 5.0

Figure 5. (a) DLS colloidal size distribution profiles for CL micelles **A** (■) and **B** (○) in aqueous solutions at pH 5.0 and 20 °C. TEM images of CL micelles **A** (b) and **B** (c) at pH 5.0 and 20 °C.

grafts in the aqueous phase for the purpose of retaining its prominent chain-segmental mobility at the expense of reduced association of polymer backbones with PNIPAAm grafts. Figure 4 shows mainly ^{1}H NMR spectra of copolymers **A** and **B** in D$_2$O (pD 5.0) at 20 and 60 °C. The fact that remarkable integral reductions in the methyl proton signals (δ 1.1 ppm) of PNIPAAm segments for both copolymers **A** and **B** were observed when temperature was increased from 20 to 60 °C verifies the development of micelles with hydrophobic cores comprising water-insoluble PNIPAAm segments. Upon solidification of PNIPAAm grafts, their proton spin–lattice relaxation times become dramatically reduced, rendering themselves undetectable by ^{1}H NMR. Nevertheless, this feature PNIPAAm signal does not fully disappear at 60 °C, indicating that the hydrophobic cores contain most likely both the solid- and liquid-like PNIPAAm regions.[26,27,38,39] The detectable fraction (40%) of the PNIPAAm segments of copolymer **B** is appreciably enhanced compared to that (29%) of **A** at 60 °C. This is because the mPEG coronas of micelles **B** reduce hydrophobic PAAc/PNIPAAm association and enhance copolymer hydration,
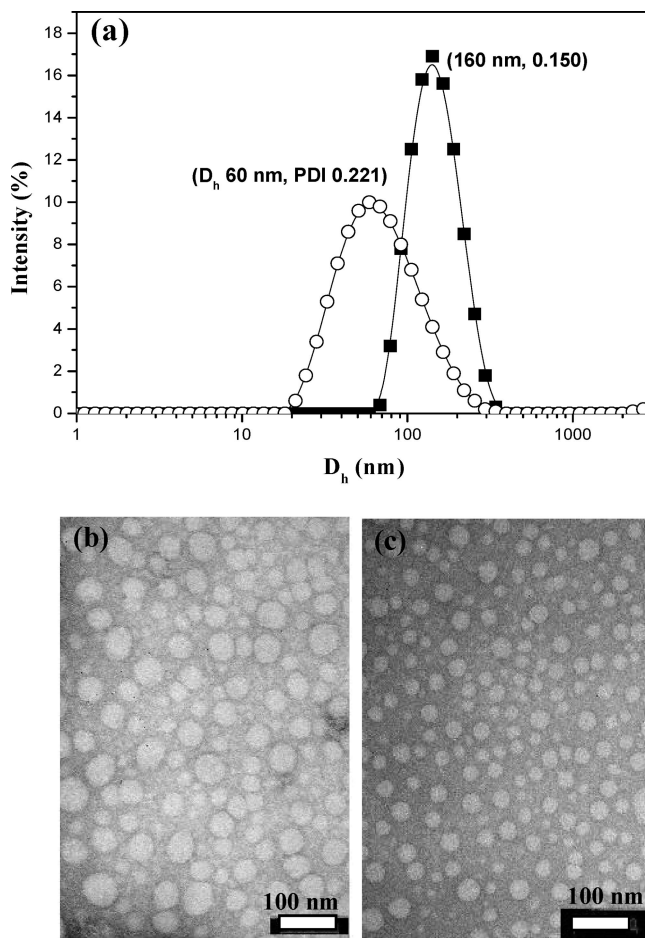
thereby rendering solidification of PNIPAAm segments more difficult. As expected, the ethylene proton signal of the mPEG grafts in copolymer **B** at 3.6 ppm is fully detectable regardless of the temperature change. It is noteworthy that, while the methyl proton signal of the MEA units of copolymer **B** at δ 1.9 ppm becomes somewhat stronger in its intensity and sharpened in its shape when temperature is increased from 20 to 60 °C due to the thermally enhanced chain-segmental mobility and the reduced heterogeneity, an appreciable reduction in the MEA signal integral for copolymer **A** is observed. This agrees with the above postulation that MEA residues are partially embedded within solidified hydrophobic cores of micelles **A**, whereas MEA moieties are apt to reside within the relatively loose AAc-rich shells of micelles **B** in the presence of mPEG grafts. Scheme 2 illustrates the thermally induced micellization of copolymers **A** and **B**, respectively.

CL Micelle Formation Mechanisms. Upon radical polymerization of the MEA residues of micelles **A** or **B** in aqueous solution (pH 5.0) using APS as the initiator at 60 °C, CL micelles were produced. This was accompanied by the full disappearance of the ^{1}H NMR feature proton signals at δ 6.1 and 5.7 ppm of the MEA residues from CL micelles in D$_2$O at 20 °C (e.g., see the spectrum for CL micelles in Figure 4). Figure 5a shows the particle size distribution profiles for both CL micelles **A** and **B** determined by DLS in aqueous solutions (pH 5.0) at 20 °C. The results indicate that the assemblies after being covalently stabilized are capable of retaining their integrity without disintegration into individual macromolecular unimers in the aqueous phase at ambient temperature. The difference in the particle size between CL micelles **A** and **B** is closely related
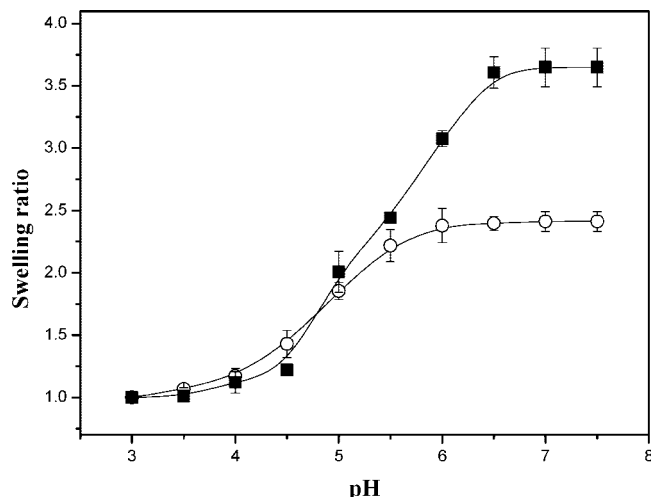
Figure 6. Swelling ratio of CL micelles **A** (■) and **B** (○) in aqueous solutions at 20 °C as a function of pH. The error bar associated with each data point represents the standard deviation of triplicate measurements.

to that between those two thermally induced micelles prior to cross-linking (Table 2). The TEM images in Figure 5b and c show that these CL micelles are in spherical shape with dried particle sizes of ca. 55 and 40 nm in diameter for CL micelles **A** and **B**, respectively. The sizes of CL micelles **A** and **B** observed by TEM are much smaller than those (130 and 60 nm in D_h for **A** and **B**, respectively) measured by DLS in the aqueous phase at pH 5.0 and 20 °C. The difference is a result of the transition of CL micelles from dried (TEM) to swollen state (DLS). Similar observations were reported in the literature.[14,23] It should be noted that, owing to the tendency of polymeric particles to spread and flatten on the copper grid in the sample preparation step, the apparent colloidal particle size distribution measured by TEM is generally broader compared to the DLS counterpart, as reported elsewhere.[40]

The response of the CL micelle size to pH change at 20 °C is illustrated in Figure 6. The swelling ratio is defined as the ratio of the mean hydrodynamic volume of CL micelles at each preset pH to that at pH 3.0, as shown by the following equation

$$\text{Swelling ratio} = \left(\frac{D_h}{D_{ho}}\right)^3$$

where D_h is the hydrodynamic diameter of CL micelles at each pH and D_{ho} is the reference hydrodynamic diameter at pH 3.0, determined by DLS. The AAc-containing hydrogel nanoparticles swell in response to an increase in the ionization of AAc units primarily due to the accumulation of freely mobile ions within cross-linked networks that induces the development of an ionic osmotic gradient and thus water influx.[41] For CL micelles **B**, the transition occurs mainly in the pH range 4.0−6.0, whereas the pH range for the volume response of **A** is slightly wider (pH 4.0−6.5). This is most likely due to the interactions of partial PAAc segments with PNIPAAm grafts within CL micelles **A**, thereby leading to more retarded AAc ionization. This will be discussed in more detail below. The DLS data further confirm the structural stability of these colloidal systems at pH 7.5 and 20 °C (Supporting Information). Nevertheless, CL micelles **A** are more susceptible than **B** in the volume transition in terms of the swelling ratio to pH change, particularly in the high pH range (Figure 6). This is in agreement with the difference in the volume transition from the dried to swollen state (pH 5.0, 20 °C) between CL micelles **A** (from 55 to 160 nm) and **B** (from 40 to 60 nm). The first and second numeric values in the parentheses represent the dried particle
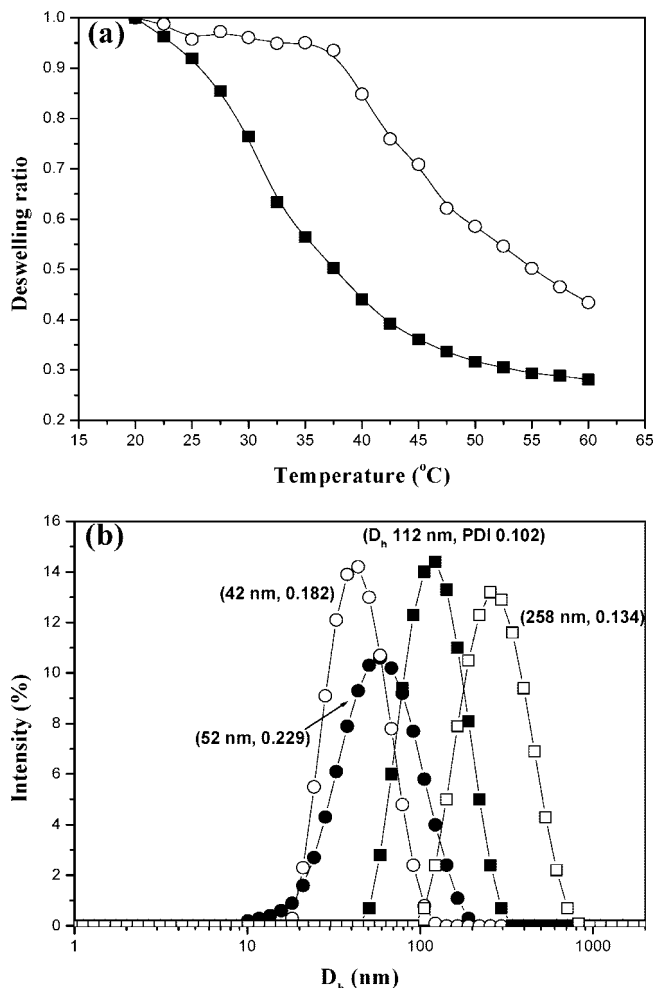

Figure 7. (a) Deswelling ratio of CL micelles **A** (■) and **B** (○) in aqueous solutions of pH 5.0 as a function of temperature. The deswelling ratio is defined herein as the ratio of the mean hydrodynamic volume of CL micelles at each temperature to that at 20 °C. (b) DLS size distribution profiles for CL micelles **A** (square) and **B** (circle) in aqueous solutions of pH 3.0 at 20 (solid) and 40 °C (open).

diameter and mean hydrodynamic diameter determined by TEM and DLS, respectively.

It has been well recognized that a hydrogel reaches its equilibrium swelling by a sole counterbalanced retractile force originating from the elastically effective chain segments within polymeric network, while the concentration of elastic chains is virtually governed by the extent of cross-linking along polymer chains.[41] Different responses of CL micelles **A** and **B** to pH change at ambient temperature is thus primarily ascribed to their varying cross-linking densities, although both copolymers **A** and **B** comprise identical amounts of MEA units. The effect of cross-linking density on the swelling of CL micelles in a similar manner was reported in the literature.[42−44] For micelles **B**, which are characterized by confinement of the MEA residues in relatively loose AAc-rich shells, radical polymerization of MEA units took place effectively and exclusively in these shell regions, thereby leading to highly shell cross-linked (SCL) micelles (Scheme 2). By contrast, owing to the entrapment of partial AAc/MEA backbones within the solidified hydrophobic cores of micelles **A**, polymerization occurs throughout the shell and core regions. As a consequence, bulk cross-linked (BCL) micelles were achieved. Comparing with SCL micelles **B**, the cross-linking density of BCL micelles **A** can be reduced to some extent as a result of the dilution of the MEA residues throughout the micellar body. The reduction in cross-linking density can become particularly pronounced in the core regions due to the

inefficient polymerization caused by the limited solubility of APS and restricted mobility of MEA units in the solidified hydrophobic PNIPAAm microdomains.

These two CL micelles also show the volume transition in response to changes in temperature (Figure 7). At pH 5.0, SCL micelles **B** commence the thermally induced volume change at an onset temperature of ca. 35 °C, indicating that the phase separation of PNIPAAm grafts occurs without significant interactions with mPEG and PAAc chain segments (Figure 7a). Nevertheless, solidification of PNIPAAm grafts in the core areas of SCL micelles led to a significant reduction in the colloidal particle size. Detailed structural characterization of SCL micelles subjected to the thermal treatment at varying pH will appear in our future report. On the other hand, the temperature-dependent volume transition profile for BCL micelles **A** (see the square data points in Figure 7a) suggests that PNIPAAm grafts, while undergoing the thermally induced solidification at pH 5.0, retain interactions with un-ionized AAc residues, rendering the onset of phase transition at temperature much lower than the LCST of PNIPAAm.[33,34] These results strongly indicate that the morphological difference between thermo-induced micelles **A** and **B** developed by the mPEG effects virtually predominates in the distinct structural responses of CL micelles to pH and temperature changes.

It is noteworthy that, at pH 3.0 where the electrostatic repulsion among colloidal particles is greatly diminished, aggregation of BCL micelles **A** occurs by the enhanced hydrophobic association with the temperature being raised from 20 to 40 °C. This led to an increase in the hydrodynamic size of the colloidal system as shown by the solid and open square data points in Figure 7b. Distinct from the aggregation behavior of BCL micelles **A**, both the size and PDI of SCL micelles **B** decrease in response to the same temperature change at pH 3.0. This illustrates an additional pronounced effect of mPEG grafts acting as highly flexible coronas on the surfaces of SCL micelles to effectively prevent particles from aggregating with one another.

Conclusion

Two graft copolymers comprising AAc and MEA units as the backbone and either PNIPAAm alone (copolymer **A**) or both PNIPAAm and mPEG (**B**) as the grafts were prepared in this study. While both the graft copolymers in the aqueous phase (pH 5.0) underwent thermally induced self-assembly into polymeric micelles, extensive interactions of un-ionized AAc residues and PNIPAAm segments occurred for copolymer **A** at ambient temperature. As a result, polymeric backbones were partially embedded within the hydrophobic PNIPAAm cores of the thermally induced micelles **A**. This then led to bulk (including both core/shell) cross-linking of micelles upon free radical polymerization of the MEA units within micellar assemblies initiated by APS at high temperature. By contrast, the thermally induced micelles **B** in the presence of mPEG as the second graft were characterized by the confinement of AAc/MEA backbones in the AAc-rich shell regions of micelles at high temperature. Radical polymerization of the MEA units of micelles took place exclusively in such shell regions, thereby leading to highly shell cross-linked micelles. Characterization of CL micelles **A** and **B** showed that their distinct responsive behaviors to pH and temperature changes were closely related to the difference in the morphological structures of these two colloidal systems, primarily as a result of the mPEG effects.

References and Notes

(1) Zhang, L.; Guo, R.; Yang, M.; Jiang, X.; Liu, B. *Adv. Mater.* **2007**, *19*, 2988–2992.
(2) Cheng, C.; Wei, H.; Zhu, J. L.; Chang, C.; Cheng, H.; Li, C.; Cheng, S. X.; Zhang, X. Z.; Zhuo, R. X. *Bioconjugate Chem.* **2008**, *19*, 1194–1201.
(3) Wang, H.; An, Y.; Huang, N.; Ma, R.; Li, J.; Shi, L. *Macromol. Rapid Commun.* **2008**, *29*, 1410–1414.
(4) Luo, S.; Xu, J.; Zhang, Y.; Liu, S.; Wu, C. *J. Phys. Chem. B* **2005**, *109*, 22159–22166.
(5) Chen, X.; An, Y.; Zhao, D.; He, Z.; Zhang, Y.; Cheng, J.; Shi, L. *Langmuir* **2008**, *24*, 8198–8204.
(6) Zhang, W.; Shi, L.; Ma, R.; An, Y.; Xu, Y.; Wu, K. *Macromolecules* **2005**, *38*, 8850–8852.
(7) Wan, S.; Jiang, M.; Zhang, G. *Macromolecules* **2007**, *40*, 5552–5558.
(8) Sundararaman, A.; Stephan, T.; Grubbs, R. B. *J. Am. Chem. Soc.* **2008**, *130*, 12264–12265.
(9) Bronich, T. K.; Keifer, P. A.; Shlyakhtenko, L. S.; Kabanov, A. V. *J. Am. Chem. Soc.* **2005**, *127*, 8236–8237.
(10) Rheingans, O.; Hugenberg, N.; Harris, J. R.; Fischer, K.; Maskos, M. *Macromolecules* **2000**, *33*, 4780–4790.
(11) Iijima, M.; Nagasaki, Y.; Okada, T.; Kato, M.; Kataoka, K. *Macromolecules* **1999**, *32*, 1140–1146.
(12) Guo, A.; Liu, G.; Tao, J. *Macromolecules* **1996**, *29*, 2487–2493.
(13) O'Reilly, R. K.; Joralemon, M. J.; Hawker, C. J.; Wooley, K. L. *New J. Chem.* **2007**, *31*, 718–724.
(14) Zhang, J.; Jiang, X.; Zhang, Y.; Li, Y.; Liu, S. *Macromolecules* **2007**, *40*, 9125–9132.
(15) Butun, V.; Billingham, N. C.; Armes, S. P. *J. Am. Chem. Soc.* **1998**, *120*, 12135–12136.
(16) Liu, S.; Weaver, J. V. M.; Save, M.; Armes, S. P. *Langmuir* **2002**, *18*, 8350–8357.
(17) Butun, V.; Wang, X. S.; de Paz Banez, M. V.; Robinson, K. L.; Billingham, N. C.; Armes, S. P.; Tuzar, Z. *Macromolecules* **2000**, *33*, 1–3.
(18) Zhang, Q.; Remsen, E. E.; Wooley, K. L. *J. Am. Chem. Soc.* **2000**, *122*, 3642–3651.
(19) Weaver, J. V. M.; Tang, Y.; Liu, S.; Iddon, P. D.; Grigg, R.; Billingham, N. C.; Armes, S. P.; Hunter, R.; Rannard, S. P. *Angew. Chem., Int. Ed.* **2004**, *43*, 1389–1392.
(20) Jiang, X.; Luo, S.; Armes, S. P.; Shi, W.; Liu, S. *Macromolecules* **2006**, *39*, 5987–5994.
(21) Xu, X.; Smith, A. E.; Kirkland, S. E.; McCormick, C. L. *Macromolecules* **2008**, *41*, 8429–8435.
(22) Li, Y.; Du, W.; Sun, G.; Wooley, K. L. *Macromolecules* **2008**, *41*, 6605–6607.
(23) Jiang, X.; Ge, Z.; Xu, J.; Liu, H.; Liu, S. *Biomacromolecules* **2007**, *8*, 3184–3192.
(24) Li, Y.; Lokitz, B. S.; McCormick, C. L. *Macromolecules* **2006**, *39*, 81–89.
(25) Dou, H.; Jiang, M.; Peng, H.; Chen, D.; Hong, Y. *Angew. Chem., Int. Ed.* **2003**, *42*, 1516–1519.
(26) Hsu, Y. H.; Chiang, W. H.; Chen, C. H.; Chern, C. S.; Chiu, H. C. *Macromolecules* **2005**, *38*, 9757–9765.
(27) Hsu, Y. H.; Chiang, W. H.; Chen, M. C.; Chern, C. S.; Chiu, H. C. *Langmuir* **2006**, *22*, 6764–6770.
(28) Pinchuk, L.; Eckstein, E. C.; van der Mark, M. R. *J. Biomed. Mater. Res.* **1984**, *18*, 671–684.
(29) Luo, S.; Xu, J.; Zhu, Z.; Wu, C.; Liu, S. *J. Phys. Chem. B* **2006**, *110*, 9132–9139.
(30) Chung, J. E.; Yokoyama, M.; Suzuki, K.; Aoyagi, T.; Sakurai, Y.; Okano, T. *Coll. Surf. B* **1997**, *9*, 37–48.
(31) Kalyanasundaram, K.; Thomas, J. K. *J. Am. Chem. Soc.* **1977**, *99*, 2039–2044.
(32) Chen, G.; Hoffman, A. S. *Nature (London)* **1995**, *373*, 49–52.
(33) Kulkarni, S.; Schilli, C.; Grin, B.; Muller, A. H. E.; Hoffman, A. S.; Stayton, P. S. *Biomacromolecules* **2006**, *7*, 2736–2741.

(34) Kokufuta, E.; Wang, B.; Yoshida, R.; Khokhlov, A. R.; Hirata, M. *Macromolecules* **1998**, *31*, 6878–6884.

(35) Koussathana, M.; Lianos, P.; Staikos, G. *Macromolecules* **1997**, *30*, 7798–7802.

(36) Holappa, S.; Kantonen, L.; Winnik, F. M.; Tenhu, H. *Macromolecules* **2004**, *37*, 7008–7018.

(37) Deo, P.; Deo, N.; Somasundaran, P.; Jockusch, S.; Turro, N. J. *J. Phys. Chem. B* **2005**, *109*, 20714–20718.

(38) Chiang, W. H.; Hsu, Y. H.; Chern, C. S.; Chiu, H. C. *J. Phys. Chem. B* **2009**, *113*, 4187–4196.

(39) Heald, C. R.; Stolnik, S.; Kujawinski, K. S.; De Matteis, C.; Garnett, M. C.; Illum, L.; Davis, S. S.; Purkiss, S. C.; Barlow, R. J.; Gellert, P. R. *Langmuir* **2002**, *18*, 3669–3675.

(40) Jones, C. D.; Lyon, L. A. *Macromolecules* **2000**, *33*, 8301–8306.

(41) Chiu, H. C.; Lin, Y. F.; Hung, S. H. *Macromolecules* **2002**, *35*, 5235–5242.

(42) Ma, Q.; Remsen, E. E.; Kowalewski, T.; Schaefer, J.; Wooley, K. L. *Nano Lett.* **2001**, *1*, 651–655.

(43) Zhang, Z.; Liu, G.; Bell, S. *Macromolecules* **2000**, *33*, 7877–7883.

(44) Liu, S.; Weaver, J. V. M.; Tang, Y.; Billingham, N. C.; Armes, S. P.; Tribe, K. *Macromolecules* **2002**, *35*, 6121–6131.